Inorganic Chemistry

Article

pubs.acs.org/IC

Formation of Ternary Complexes with MgATP: Effects on the Detection of Mg^{2+} in Biological Samples by Bidentate Fluorescent Sensors

Sarina C. Schwartz, Brismar Pinto-Pacheco, Jean-Philippe Pitteloud, and Daniela Buccella*

Department of Chemistry, New York University, New York, New York 10003

Supporting Information

ABSTRACT: Fluorescent indicators based on β-keto-acid bidentate coordination motifs display superior metal selectivity profiles compared to current *o*-aminophenol-*N*,*N*,*O*-triacetic acid (APTRA) based chelators for the study of biological magnesium. These low denticity chelators, however, may allow for the formation of ternary complexes with Mg^{2+} and common ligands present in the cellular milieu. In this work, absorption, fluorescence, and NMR spectroscopy were employed to study the interaction of turn-on and ratiometric fluorescent indicators based on 4-oxo-4H-quinolizine-3-carboxylic acid with Mg^{2+} and ATP, the most abundant chelator of biological magnesium, thus revealing the formation of ternary complexes under conditions relevant to fluorescence imaging. The formation of ternary species elicits comparable or greater optical changes than those attributed to the formation of binary complexes alone. Dissociation of the fluorescent indicators from both ternary and binary species have apparent equilibrium constants in the low millimolar range at pH 7 and 25 °C. These results suggest that these bidentate sensors are incapable of distinguishing between free Mg^{2+} and MgATP based on ratio or intensity-based steady-state fluorescence measurements, thus posing challenges in the interpretation of results from fluorescence imaging of magnesium in nucleotide-rich biological samples.

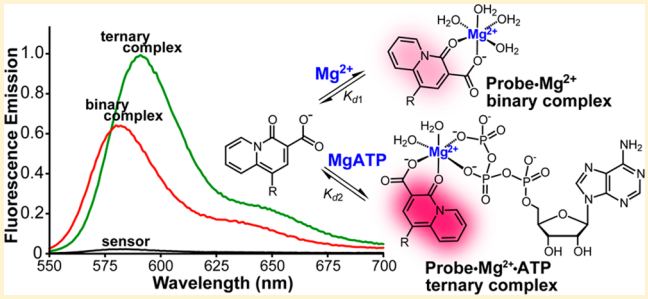

INTRODUCTION

Magnesium is the most abundant divalent cation in the cell, with numerous roles that are essential for cellular function.[1−3] The estimated total concentration of Mg^{2+} in mammalian cells varies between 14 and 20 mM, the majority of it bound to ATP and a lesser extent to proteins, phospholipids, and various phosphometabolites.[4] The concentration of *free* cytosolic magnesium, $[Mg^{2+}]_i$, not associated with macromolecules, is estimated to be in the sub-millimolar range.[4,5] Abnormal levels of magnesium are associated with a number of age-related and neuronal diseases ranging from hypertension to Alzheimer's disease. The mechanisms by which Mg^{2+} concentration is regulated at the cellular level and the implications in human health, however, remain poorly understood due to the scarcity of efficient chemical tools for the study of this ion. Most detection methods employed thus far do not offer the combination of selectivity and spatiotemporal resolution required to study magnesium in the complex chemical environment offered by the cell.

The use of fluorescent indicators has emerged as a powerful approach to detect free magnesium in biological samples.[6−8] Most fluorescent indicators available commercially at this time are based on *o*-aminophenol-*N*,*N*,*O*-triacetic acid (APTRA) chelators (Figure 1),[9] which afford a rapid response and dissociation constant in the low millimolar range, optimal for measurements of free Mg^{2+}.[9] Nevertheless, the APTRA binding group suffers from low selectivity against Ca^{2+} and Zn^{2+} (e.g., $K_{d,Ca^{2+}}$ = 20 μM and $K_{d,Zn^{2+}}$ = 11 nM for Mag-fura-2),[10] which may give rise to artifacts in the detection of Mg^{2+} in the cellular milieu. Alternative chelators based on β-keto-acids and related β-dicarbonyl bidentate binding motifs have been incorporated recently into fluorescent probes for the detection of Mg^{2+}.[7,11−14] Significantly, these chelators form magnesium complexes with typical dissociation constants in the low millimolar range and exhibit dissociation constants the same or 1 order of magnitude higher when complexed to Ca^{2+}. As a result, they are practically insensitive to biological concentrations of Ca^{2+} and show great promise for the development of fluorescent probes with an improved metal selectivity profile for biological applications. Unlike the pentadentate APTRA-based sensors, β-dicarbonyl species may occupy only two sites in the coordination sphere of Mg^{2+}, leaving room for coordination of further charged or neutral ligands and formation of ternary species. The formation of these species and its effect in the performance of fluorescent sensors have been long overlooked and warrant further investigation. In this paper, we provide evidence for the formation of ternary complexes from interaction of bidentate fluorescent indicators with MgATP, the most abundant form of bound Mg^{2+} in the cell, and

Received: January 9, 2014
Published: March 4, 2014

   dx.doi.org/10.1021/ic5000606 | *Inorg. Chem.* 2014, 53, 3204−3209

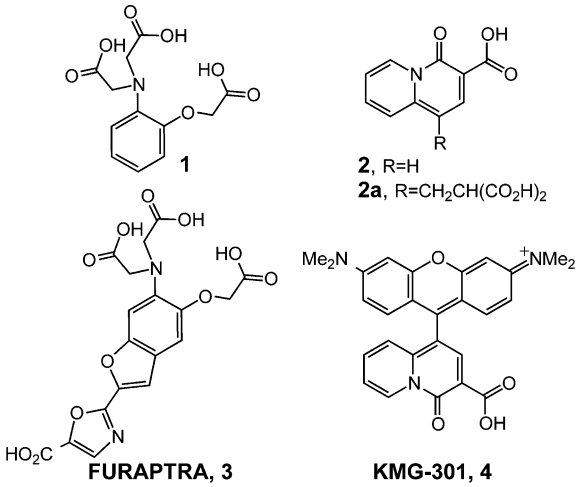

Figure 1. Magnesium-binding chelators *o*-aminophenol-*N*,*N*,*O*-triacetic acid (APTRA, **1**) and 4-oxo-4H-quinolizine-3-carboxylic acid (**2**) employed in the design of fluorescent probes such as FURAPTRA (Mag-Fura-2, **3**) and KMG-301 (**4**) for imaging of Mg^{2+}.

investigate its effect on the optical properties of the indicators under conditions relevant to fluorescence imaging of biological magnesium.

EXPERIMENTAL SECTION

Materials and Methods. Compounds KMG-301,[7] **2**,[15] and **2a**[15] were prepared according to reported procedures, and their purity (>98%) was verified by reverse phase C-18 HPLC. High-purity piperazine-*N*,*N*′-bis(2-ethanesulfonic acid) (PIPES), 37% HCl, 45% KOH, and 99.999% anhydrous $MgCl_2$ were purchased from Aldrich. High purity 99.999% KCl was obtained from Alfa Aesar. ATP was obtained from Aldrich as the disodium salt. Deuterium oxide (D, 99.9%), sodium deuteroxide (D, 99.5%, 40% w/w in D_2O), and deuterium chloride (D, 99.5%, 35% w/w in D_2O) were obtained from Cambridge Isotope Laboratories. All aqueous solutions for fluorescence experiments were prepared using deionized water having a resistivity of ≥18 MΩ/cm. Other solvents were obtained from commercial suppliers and used as received. Aqueous buffers were treated with Chelex resin (Bio-Rad) according to the manufacturer's protocol to remove adventitious metal ions.

Fluorescence Spectroscopic Methods. Fluorescence spectra were acquired on a QuantaMaster 40 Photon Technology International spectrofluorometer equipped with xenon lamp source, emission and excitation monochromators, excitation correction unit, and PMT detector. Emission spectra were corrected for the detector wavelength-dependent response. The excitation spectra were corrected for the wavelength-dependent lamp intensity. All measurements were conducted at 25.0 ± 0.1 °C controlled with Quantum Northwest cuvette holders. Fluorescence measurements at pH 7.0 were conducted in aqueous buffer containing 50 mM PIPES and 100 mM KCl. Stock solutions of compounds **2** and **2a**, 1.0 mM, were prepared in PIPES buffer at pH 7.0. Stock solutions of KMG-301, 1.0 mM, were prepared in DMSO. All stock solutions for fluorescence measurements were stored at −20 °C in 20−200 μL aliquots and thawed immediately before each experiment. Excitation for compound **2** was provided at 385 nm and for compound **2a** at 395 nm. Excitation for KMG-301 was provided at 540 nm, and corrected emission spectra were integrated in the 545−750 nm range. Apparent K_d values for a 1:1 binding model (probe/Mg^{2+} or probe/MgATP) were obtained from nonlinear fit of integrated florescence intensity or fluorescence ratio plots (see Supporting Information for details).

NMR Spectroscopy Studies. NMR spectroscopic data were acquired on a Bruker AVANCE-400 NMR or Bruker AVANCE III-600 NMR spectrometer equipped with a 5 mm sample diameter Inverse Quadruple Resonance Probe. ^1H NMR shifts were calibrated based on the protio impurity of the solvent peak. Changes of the chemical shift of the indicator's protons as a function of total magnesium concentration were fitted using a model including two sequential dissociation equilibria as described in the Supporting Information. Diffusion measurements were conducted on a Bruker AVANCE III-600 NMR using the ledbpgp2s pulse program,[16] with a longitudinal eddy current delay of 5 ms, diffusion time Δ = 100 ms, and effective gradient duration δ = 3600 μs. The 90 deg RF pulse was calibrated for each sample. Temperature was held at 25 °C throughout the experiment. The gradient power of the probe was calibrated from the diffusion coefficient of water. Diffusion experiments were run with 16, 32, or 64 scans; more scans were used for samples with broad peaks (concentrations of MgATP above 10 mM). Linear gradient strength ramps from 8% to 50% were employed for samples of sensors **2** and **2a** with and without Mg^{2+}. Gradient ramps of 8 to 45% were employed for samples treated with MgATP. The intensities of non-overlapping peaks were analyzed using the relaxation module in the Bruker Topspin version 3.2 software (Supporting Information). Diffusion coefficients are reported as averages of the values obtained from analysis of the different peaks corresponding to one given compound.

Samples for NMR spectroscopy were prepared by mixing appropriate amounts of Na_2ATP and $MgCl_2$ solutions in D_2O with a sensor stock solution containing Tris buffer in D_2O.[17] The mixture was adjusted to pD 7.40[18] with small amounts of 37% DCl in D_2O, and diluted to a final concentration of 2.5 mM compound **2** in 10 mM Tris or 5.0 mM compound **2a** in 25 mM Tris. Na_2ATP was added from a 100 mM stock solution in D_2O, adjusted to pD 7.40 with NaOD. Magnesium was added from 100 mM or 1.00 M stock solutions prepared by dissolving high purity anhydrous $MgCl_2$ beads in D_2O. Representative samples were checked for pD changes after mixing.

X-ray Diffraction Studies. Crystals of $[\mathbf{2}]_2Mg(OH_2)_2$ were obtained as follows: A 25 mM solution of chelator **2** in DMSO (50 μL) at 60 °C was treated with aqueous PIPES buffer at pH 7.0 containing 50 mM $MgCl_2$ (250 μL), layered atop the first solution. The warm mixture was allowed to cool slowly and diffuse over a period of 16 h protected from light. Single crystals suitable for X-ray analysis were coated with Paratone-N oil and mounted on fiber loops for analysis. Diffraction data were collected at 100(2) K on a Bruker APEXII CCD X-ray diffractometer performing φ scans using graphite-monochromated Mo Kα radiation. Structure was solved by direct methods and standard difference map techniques and was refined by full-matrix least-squares procedures on F^2 with SHELXTL (version 6.12).[19] Crystallographic data collection and refinement parameters are summarized in Table S1, Supporting Information.

RESULTS AND DISCUSSION

Levy and co-workers developed a series of 4-oxo-4H-quinolizine-3-carboxylic acid derivatives (Figure 1) that bind Mg^{2+} with dissociation constants in the low millimolar range and show negligible response to Ca^{2+}.[15] Based on these chelators, Oka's group developed fluorescein and rosamine fluorescent compounds KMG-104[13] and KMG-301[7] that perform as turn-on sensors with excitation and emission in the visible range. In our study, we first employed the most recently reported rosamine probe, KMG-301, as a representative example of a bidentate dicarbonyl-based chelator that would allow us to investigate the formation of ternary complexes in conditions akin to those employed in fluorescence bioimaging experiments.

Treatment of KMG-301 with increasing Mg^{2+} concentrations in aqueous buffer at pH 7.0 leads to an increase in the fluorescence emission (Figures 2 and S1) for an overall ∼24-fold turn on.[20] Nonlinear fit of the integrated fluorescence as a function of magnesium concentration, obtained under our experimental conditions, results in an apparent dissociation

dx.doi.org/10.1021/ic5000606 | Inorg. Chem. 2014, 53, 3204−3209

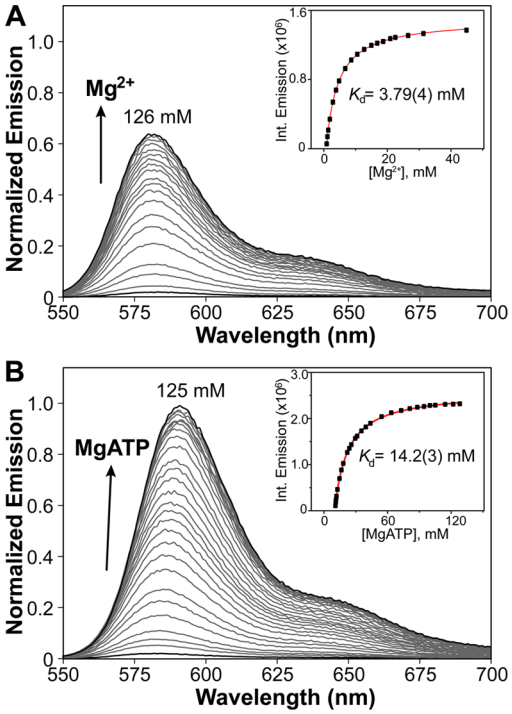

Figure 2. Fluorescence emission of 1.0 μM solutions of KMG-301 in response to increasing concentrations of Mg^{2+} (A) or MgATP complex (B). Titrations were conducted in 50 mM aqueous PIPES buffer, 100 mM KCl, pH 7.0, 25 °C. Excitation wavelength λ_{ex} = 540 nm. Insets correspond to the integrated emission (squares) and nonlinear fit (red line) as a function of [Mg^{2+}] or [MgATP] using a 1:1 binding model.

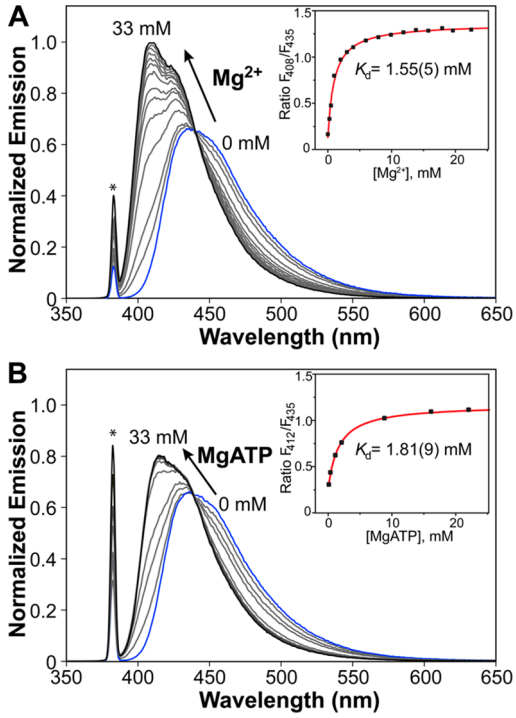

Figure 3. Fluorescence emission of 1.0 μM solutions of 4-oxo-4H-quinolizine-3-carboxylate, compound **2**, in response to increasing concentrations of Mg^{2+} (A) or MgATP complex (B). All titrations were conducted in 50 mM PIPES buffer, 100 mM KCl, pH 7.0, 25 °C. Excitation wavelength λ_{ex} = 385 nm (* = scattered excitation light). Insets correspond to the ratio of fluorescence intensity at two wavelengths, F_{408}/F_{435} (F_{412}/F_{435} for MgATP titration, squares) and nonlinear fit (red line) as a function of added magnesium or MgATP using a 1:1 binding model.

constant K_d = 3.79 ± 0.04 mM for the 1:1 complex of the chelator with Mg^{2+} at 25 °C. Significantly, a titration employing increasing concentrations of Mg^{2+} as a 1:1 complex with ATP (Figure 2b), leads to a ∼58% larger increase in emission intensity compared to that observed in the titration with $MgCl_2$ over the same concentration range. The intensity increase is accompanied by a slight red shift in the fluorescence maximum. A control experiment conducted with the addition of ATP, in the absence of Mg^{2+} (Figure S1, Supporting Information), shows a similar red shift but only a slight increase in the fluorescence intensity, thus supporting the notion that the fluorescence turn on in each case involves magnesium coordination. Nonlinear fit of the binding isotherm for the titration with MgATP yields an apparent dissociation constant K_d = 14.2 ± 0.3 mM at 25 °C for a 1:1 binding model. A similar value is obtained for a titration conducted in the presence of a 1:2 ratio Mg^{2+} to ATP (data not shown). With an apparent dissociation constant in the mid-micromolar range for MgATP under physiological conditions,[21] the quinolizine-based chelator is not expected to displace the ATP from the coordination sphere of magnesium. Accordingly, the formation of a ternary ATP·Mg^{2+}·probe species is the most likely origin of the observed changes in fluorescence.

We also investigated the interaction between MgATP and the simpler 4-oxo-4H-quinolizine-3-carboxylate chelator **2**. Unlike KMG-301, compound **2** is fluorescent in both Mg^{2+}-free and -bound states,[15] which facilitates the study of the binding process and allows for ratiometric determination of Mg^{2+}. Treatment of **2** with increasing Mg^{2+} concentrations in aqueous buffer at pH 7.0 (Figure 3A) led to a blue shift in the fluorescence emission maximum, from 435 to 408 nm. The ratio of emission at these two wavelengths, F_{408}/F_{435}, was employed to calculate an apparent dissociation constant, which resulted in a value of K_d = 1.55 ± 0.05 mM for the 1:1 complex of the chelator with Mg^{2+} under our experimental conditions. Treatment of **2** with increasing concentrations of MgATP over the same range (Figure 3B) also led to a blue shift in the fluorescence emission maximum, from 435 to 412 nm. Employing the ratio of emission at these two wavelengths, F_{412}/F_{435}, an apparent constant K_d = 1.81 ± 0.09 mM for the dissociation of the fluorescent probe from a 1:1:1 ATP·Mg^{2+}·probe ternary complex was obtained. A control experiment conducted with the addition of ATP in the absence of Mg^{2+} only led to a slight decrease in the fluorescence of the sensor with no significant blue shift (data not shown), presumably due to mild quenching effect of the purine base. Therefore, the wavelength shift observed in the presence of MgATP can be attributed to coordination of the magnesium center to the bidentate chelator.

The apparent affinities of **2** for Mg^{2+} and MgATP are surprisingly similar and, in comparison to those of the rosamine probe KMG-301, indicate that the xanthene moiety has an electronic effect on the apparent binding properties of the chelator. With either sensor, however, the MgATP-induced optical changes are expected to contribute significantly to the overall fluorescence response obtained in cell or tissue imaging experiments. This contribution cannot be neglected in the interpretation of imaging studies of Mg^{2+}, as it does not allow for a clear distinction between the detection of free Mg^{2+} from

dx.doi.org/10.1021/ic5000606 | Inorg. Chem. 2014, 53, 3204−3209

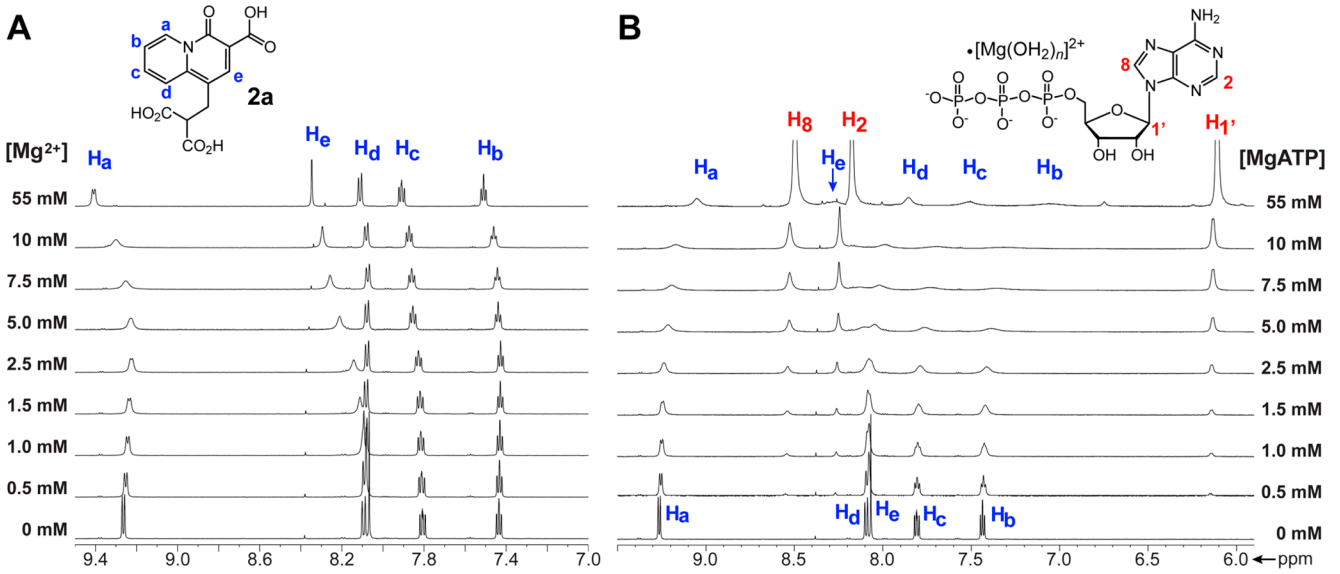

Figure 4. ^{1}H NMR spectra (600 MHz, D_2O, 25 mM Tris buffer, pD = 7.40, 25 °C) of a 5.0 mM solution of chelator **2a** after treatment with increasing concentrations of $MgCl_2$ (A) or MgATP (B).

its nucleotide-bound forms at typical physiological levels, based on steady state fluorescence intensity or ratio measurements. In short, the *β*-dicarbonyl-based sensors tested herein *do not* report on levels of free Mg^{2+}, as presumed in previous studies, but their optical response may reflect changes in concentration of various forms of Mg^{2+} (e.g. free + nucleotide bound).[22] This limitation may affect the performance of other low-denticity chelators and must be considered carefully.

Ternary complexes with MgATP have been reported for a variety of amines.[23−26] However, the role of Mg^{2+} in mediating the interaction is not clear in every case. The use of other metals such as Zn and Cu has allowed for the isolation and structural characterization of various ternary complexes in which the phosphate backbone of the nucleotide and a second chelator share the coordination sphere of the metal center;[25,27] similar magnesium-containing ternary complexes with fluorescent chelators are not unlikely. To gain further insight into the interaction of the fluorescent probe with MgATP, we investigated the complex formation by NMR spectroscopy (Figure 4). For this purpose, we employed a derivative of **2**, 1-(2,2-dicarboxyethyl)-4-oxo-4H-quinolizine-3-carboxylic acid **2a**, which displays similar fluorescence response to both Mg^{2+} and MgATP (Figure S2, Supporting Information) but offers increased solubility in water compared to **2**.[15] Treatment of a 5.0 mM solution of compound **2a** in aqueous buffer with increasing concentrations of Mg^{2+} reveals a gradual shift and broadening of the aromatic signals, which sharpen at high concentrations of Mg^{2+} (Figure 4A). Analysis of the chemical shift as a function of total magnesium concentration suggests at least two metal-binding steps, and a model considering the formation of both 2:1 and 1:1 chelator/Mg^{2+} species provides the best fit (Figure 5 and Supporting Information). From this analysis, two apparent dissociation constants are obtained, one of K_{d1} = 12 ± 1 mM for the chelator dissociation from the 2:1 complex, and the second K_{d2} = 0.9 ± 0.3 mM for the dissociation of the 1:1 species. The latter is consistent with the apparent dissociation constant determined by fluorescence.

The limited water solubility of the simple chelator **2** at millimolar concentrations facilitated the isolation and structural characterization of the complex $[\mathbf{2}]_2Mg(OH_2)_2$, as shown in

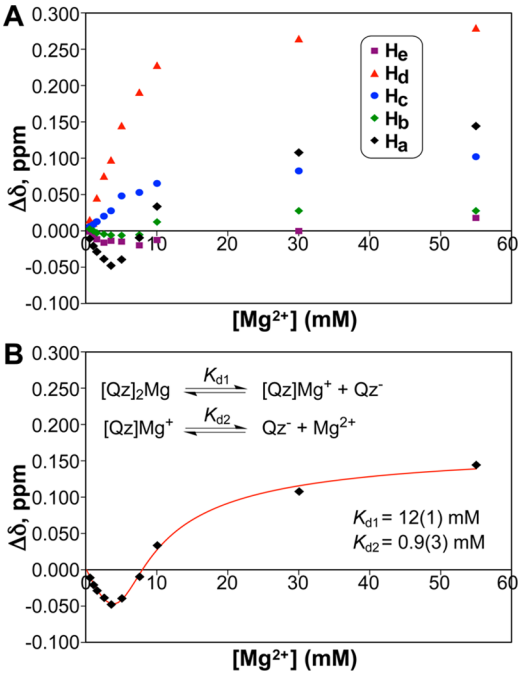

Figure 5. (A) Changes in chemical shift of aromatic protons of chelator **2a** (5.0 mM in D_2O, 25 mM Tris buffer, pD = 7.40, 25 °C) as a function of total concentration of magnesium, obtained from the ^{1}H NMR spectroscopic titrations. (B) Nonlinear fit of the changes in chemical shift for H_a in response to increasing concentrations of magnesium, employing a model that includes both the formation of complexes with 2:1 and 1:1 chelator-to-Mg^{2+} stoichiometry. Qz = quinolizine-based chelator **2a**.

Figure 6. The solid-state structure exposes a κ^2-$[O_2]$ coordination mode for two of the quinolizine-derived fluorophores forming almost perpendicular six-membered chelates around a pseudo-octahedral magnesium center. The concentration of this 2:1 chelator/Mg^{2+} species in solution is negligible at the low chelator concentration and high $[Mg^{2+}]$/[chelator] ratio involved in typical fluorescence sensing experiments. Its formation at high concentrations, however,

dx.doi.org/10.1021/ic5000606 | Inorg. Chem. 2014, 53, 3204−3209

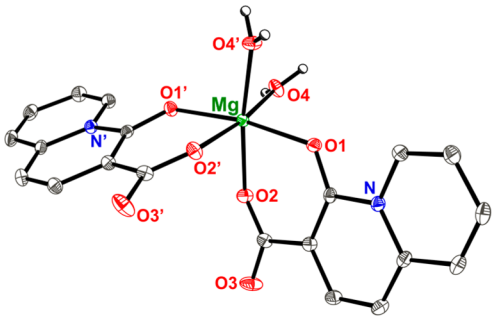

Figure 6. Molecular structure of $[\mathbf{2}]_2Mg(OH_2)_2$. ORTEP drawing with 50% probability thermal ellipsoids.

illustrates the ability of small low-denticity chelators to share the coordination sphere with other multidentate ligands, such as another molecule of **2** or potentially a biologically relevant ligand such as ATP.

A second titration experiment was conducted with a 5.0 mM solution of compound **2a** in aqueous buffer treated with increasing concentrations of MgATP and followed by ^{1}H NMR and ^{31}P NMR spectroscopy (Figures 4B and S10 and S11, Supporting Information). With the exception of the signal corresponding to proton H_e, all the aromatic signals of compound **2a** shift upfield in the ^{1}H NMR spectrum indicating the formation of a complex that is electronically different from that formed upon treatment of the chelator with $MgCl_2$ alone. Furthermore, these signals remain broad even at close-to-saturating concentrations of MgATP, likely due to the effect of conformational changes of the ATP ligand in a ternary complex.

Further evidence for the formation of ternary species upon interaction of the bidentate fluorescent probes with MgATP was obtained through NMR diffusion studies. Specifically, the translational self-diffusion coefficient of quinolizine-based chelator **2a** was determined via pulsed gradient spin–echo (PGSE) diffusion ^{1}H NMR spectroscopy experiments[16,28] in the absence and presence of near-saturating concentrations of Mg^{2+} or MgATP (Table 1). Upon treatment with $MgCl_2$, the diffusion coefficient of the chelator decreases, thus reflecting an increase in the overall size of the molecule as a result of metal complexation. The change in diffusion coefficient is, however, more pronounced upon treatment with MgATP. At high concentration of the nucleotide-bound magnesium source, the diffusion coefficient of the chelator drops to a value lower than that obtained upon complexation with magnesium and even lower than that of MgATP alone, thus consistent with the formation of a larger species. Additionally, a marked decrease in diffusion coefficient was observed for chelator **2** in the presence of MgATP (Table S2, Supporting Information); the low solubility of the compound in the presence of high concentration of magnesium, however, prevented further studies.

Table 1. Self-Diffusion Coefficients of Chelator 2a in the Presence of Various Magnesium Sources Measured by PGSE Diffusion ^{1}H NMR Spectroscopy

sample	D, 10^{-10} m^2 s^{-1}
chelator **2a**[a]	3.95(3)
chelator **2a** saturated with MgATP (40 mM)[a]	2.8(2)[c]
chelator **2a** saturated with Mg^{2+} (30 mM)[a]	3.52(4)
MgATP[b]	3.13(3)

[a]Samples containing 5.0 mM of chelator 2a in D_2O, with 25 mM Tris buffer adjusted to pD = 7.40, 25 °C. [b]Sample containing 10 mM MgATP in Tris buffer adjusted to pD = 7.40, 25 °C. [c]At 55 mM MgATP, the coefficient is, within error, the same as the coefficient at 40 mM. The broad peaks at high MgATP concentrations result in larger variance.

CONCLUSION

Much of our understanding of metal homeostasis and its implications in health and disease stems from the use of fluorescent metal indicators that enable optical tracking of ion accumulation and fluxes in the complex matrix provided by the cell. Sensor development endeavors typically devote substantial effort to the fine-tuning of dissociation constants as to provide maximum dynamic range, avoid competitive binding of other metals, and prevent displacement of typical biological chelators, thereby enabling the selective detection of the *free* or *ionized* forms of the cation under physiological conditions. Our results highlight the need for a deeper understanding of the coordination properties of the chelator, and the consideration of binding schemes beyond the simple formation of binary species, to provide a more complete depiction of the "selectivity" of fluorescent metal chelators.

We hereby provide spectroscopic evidence for the formation of ternary complexes from *β*-keto-acid fluorescent chelators, namely, 4-oxo-4H-quinolizine-3-carboxylic acid and KMG-301, with MgATP, the most abundant bound form of biological magnesium. The formation of such ternary species elicits comparable or greater optical changes than those attributed to the formation of binary complexes alone, with equilibrium constants that are similar for the binding of the chelator to either free magnesium or its nucleotide complex. As a result, these low-denticity chelators do not afford a clear distinction between free (ionized) Mg^{2+} and MgATP from simple ratio- or intensity-based steady-state fluorescence measurements. Instead, they may co-report various magnesium-containing species, thus posing challenges in the interpretation of results obtained from fluorescence imaging of magnesium in nucleotide-rich biological samples. Being a consequence of the mismatch between the typical coordination number of Mg^{2+} and the denticity of the sensor, the formation of ternary complexes is likely to influence the performance of other low-denticity chelators and must be considered carefully.

ASSOCIATED CONTENT

Supporting Information

X-ray crystallographic data in CIF format, absorption and fluorescence data for KMG-301 and chelator **2a** in the presence of Mg^{2+} or MgATP, NMR spectroscopy data for chelators **2** and **2a** in the presence of MgATP or $MgCl_2$, determination of apparent dissociation constants from NMR and fluorescence titration data, and ^{1}H PGSE NMR diffusion coefficients for compound **2**. This material is available free of charge via the Internet at http://pubs.acs.org.

AUTHOR INFORMATION

Corresponding Author

*E-mail: dbuccella@nyu.edu.

Notes

The authors declare no competing financial interest.

dx.doi.org/10.1021/ic5000606 | Inorg. Chem. 2014, 53, 3204–3209

■ ACKNOWLEDGMENTS

This research was supported in part by start-up funds granted to D.B. by New York University. B.P.-P. acknowledges the MARC Program from the National Institutes of Health for funds granted to UPRRP, Grant 5T34TGM007821-33. Dr. Chin Lin and Eli Bendet-Taicher are thanked for assistance with the setup of PGSE NMR diffusion experiments. The Bruker Avance-400 NMR spectrometer was acquired through the support of the National Science Foundation under Award Number CHE-01162222. The Bruker AVANCE III-600 NMR spectrometer was acquired through the support of New York University. The Bruker AXS SMART APEXII single crystal diffractometer was acquired through the support of the Molecular Design Institute in the Department of Chemistry at New York University.

■ REFERENCES

(1) Romani, A. *Arch. Biochem. Biophys.* **2007**, *458*, 90.
(2) Cowan, J. A. *Biometals* **2002**, *15*, 225.
(3) Sreedhara, A.; Cowan, J. A. *Biometals* **2002**, *15*, 211.
(4) Romani, A. M. P. *Arch. Biochem. Biophys.* **2011**, *512*, 1.
(5) Grubbs, R. D. *Biometals* **2002**, *15*, 251.
(6) Trapani, V.; Schweigel-Rontgen, M.; Cittadini, A.; Wolf, F. I. In *Methods Enzymol.*; Conn, P. M., Ed.; Academic Press: 2012; Vol. *505*, p 421.
(7) Shindo, Y.; Fujii, T.; Komatsu, H.; Citterio, D.; Hotta, K.; Suzuki, K.; Oka, K. *PLoS One* **2011**, *6*, e23684.
(8) (a) Fujii, T.; Shindo, Y.; Hotta, K.; Citterio, D.; Nishiyama, S.; Suzuki, K.; Oka, K. *J. Am. Chem. Soc.* **2014**, *136*, 2374. (b) Dong, X.; Han, J. H.; Heo, C. H.; Kim, H. M.; Liu, Z.; Cho, B. R. *Anal. Chem.* **2012**, *84*, 8110. (c) Marraccini, C.; Farruggia, G.; Lombardo, M.; Prodi, L.; Sgarzi, M.; Trapani, V.; Trombini, C.; Wolf, F. I.; Zaccheroni, N.; Iotti, S. *Chem. Sci.* **2012**, *3*, 727. For a review of other relevant efforts in the area, see (d) Trapani, V.; Farruggia, G.; Marraccini, C.; Iotti, S.; Cittadini, A.; Wolf, F. I. *Analyst* **2010**, *135*, 1855.
(9) Levy, L. A.; Murphy, E.; Raju, B.; London, R. E. *Biochemistry* **1988**, *27*, 4041.
(10) Hyrc, K. L.; Bownik, J. M.; Goldberg, M. P. *Cell Calcium* **2000**, *27*, 75.
(11) Suzuki, Y.; Komatsu, H.; Ikeda, T.; Saito, N.; Araki, S.; Citterio, D.; Hisamoto, H.; Kitamura, Y.; Kubota, T.; Nakagawa, J.; Oka, K.; Suzuki, K. *Anal. Chem.* **2002**, *74*, 1423.
(12) Shoda, T.; Kikuchi, K.; Kojima, H.; Urano, Y.; Komatsu, H.; Suzuki, K.; Nagano, T. *Analyst* **2003**, *128*, 719.
(13) Komatsu, H.; Iwasawa, N.; Citterio, D.; Suzuki, Y.; Kubota, T.; Tokuno, K.; Kitamura, Y.; Oka, K.; Suzuki, K. *J. Am. Chem. Soc.* **2004**, *126*, 16353.
(14) Kim, H. M.; Yang, P. R.; Seo, M. S.; Yi, J.-S.; Hong, J. H.; Jeon, S.-J.; Ko, Y.-G.; Lee, K. J.; Cho, B. R. *J. Org. Chem.* **2007**, *72*, 2088.
(15) Otten, P. A.; London, R. E.; Levy, L. A. *Bioconjugate Chem.* **2001**, *12*, 203.
(16) Wu, D. H.; Chen, A. D.; Johnson, C. S. *J. Magn. Reson. A* **1995**, *115*, 260.
(17) Tris buffer displays a simple ^{1}H NMR spectrum that causes little overlap with other resonance signals of interest and has been employed successfully in NMR spectroscopy studies of MgATP, showing no interaction with other compounds under study. See ref 24.
(18) Glasoe, P. K.; Long, F. A. *J. Phys. Chem.* **1960**, *64*, 188.
(19) Sheldrick, G. *Acta Crystallogr.* **2008**, *A64*, 112.
(20) Differences in experimental conditions may be responsible for a higher background fluorescence and smaller turn-on response compared to previously reported values. See ref 7.
(21) The dissociation equilibrium of MgATP has been studied extensively at various temperatures, pH values, and ionic strengths, resulting in a range of apparent dissociation constants that vary depending on exact experimental conditions and methods. For a review of dissociation constants, see Günther, T. *Magnes. Res.* **2006**, *19*, 225.
(22) Studies conducted on the ZnAF family of zinc-selective indicators have shown that formation of ternary complexes with various low-molecular weigth ligands may influence the optical response obtained with the indicators. See Staszewska, A.; Kurowska, E.; Bal, W. *Metallomics* **2013**, *5*, 1483.
(23) Meksuriyen, D.; Fukuchi-Shimogori, T.; Tomitori, H.; Kashiwagi, K.; Toida, T.; Imanari, T.; Kawai, G.; Igarashi, K. *J. Biol. Chem.* **1998**, *273*, 30939.
(24) Lüthi, D.; Günzel, D.; McGuigan, J. A. S. *Exp. Physiol.* **1999**, *84*, 231.
(25) Cini, R. *Comments Inorg. Chem.* **1992**, *13*, 1.
(26) Sigel, H. *Pure Appl. Chem.* **2004**, *76*, 375.
(27) Cini, R.; Bozzi, R. *J. Inorg. Biochem.* **1996**, *61*, 109.
(28) Stejskal, E. O.; Tanner, J. E. *J. Chem. Phys.* **1965**, *42*, 288.